Electronic Supplementary Material (ESI) for Dalton Transactions.

Supporting Information

Cyclometalated iridium(III) tetrazine complexes for mitochondria-targeted two-photon photodynamic therapy

Zanru Tan,‡[a] Mingwei Lin,‡[a] Jiangping Liu,*[b] Huihui Wu,*[c] and Hui Chao*[a,d]

[a] *MOE Key Laboratory of Bioinorganic and Synthetic Chemistry, Guangdong Basic Research Center of Excellence for Functional Molecular Engineering, School of Chemistry, Sun Yat-Sen University, Guangzhou, 510275, P. R. China. Email: ceschh@mail.sysu.edu.cn*

[b] *The Institute of Flexible Electronics (IFE, Future Technologies), Xiamen University, Xiamen, 361102, P. R. China. Email: liujping@xmu.edu.cn*

[c] *Department of Dermatology, The East Division of the First Affiliated Hospital, Sun Yat-Sen University, Guangzhou, 510700, P. R. China. Email: cometvivi@126.com*

[d] *MOE Key Laboratory of Theoretical Organic Chemistry and Functional Molecule, School of Chemistry and Chemical Engineering, Hunan University of Science and Technology, Xiangtan, 400201, P. R. China*

‡ These authors contributed equally to this work.

Table of Contents

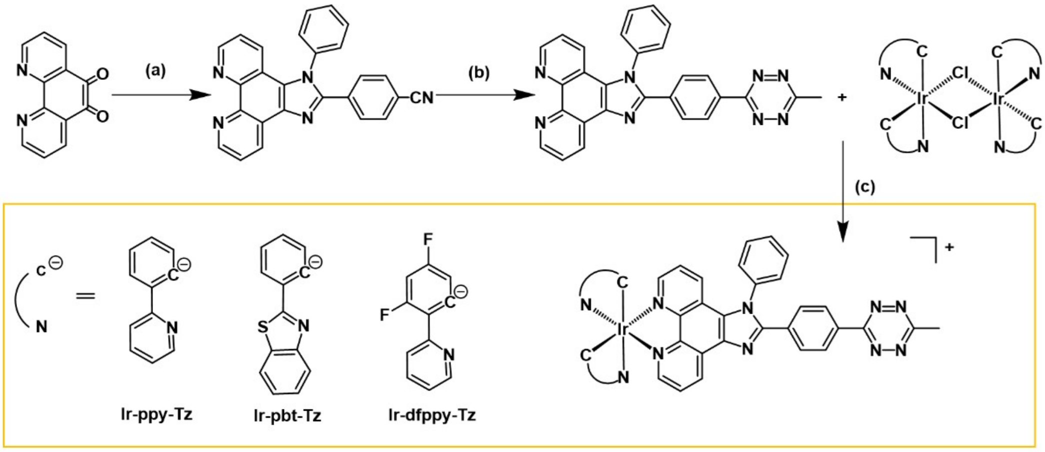

Fig. S1 Synthetic route of the iridium(III) complexes. (a) 4-cyanobenzaldehyde, aniline, NH_4OAc, HOAc, 120 °C, 12 h; (b) MeCN, $N_2H_4 \cdot H_2O$, $Zn(TOf)_2$, dioxane, Ar, 85 °C, 24 h; (c) $CHCl_3$/MeOH(1:1, v/v), Ar, 85 °C, 6 h.

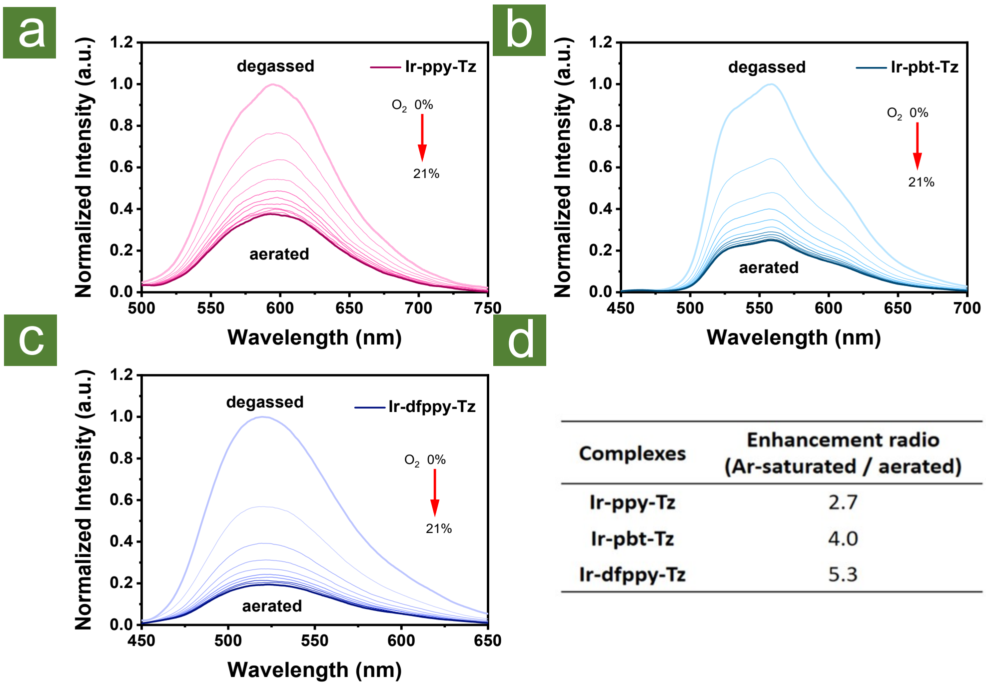

Complexes	Enhancement radio (Ar-saturated / aerated)
Ir-ppy-Tz	2.7
Ir-pbt-Tz	4.0
Ir-dfppy-Tz	5.3

Fig. S2 The emission spectra (λ_{ex} = 405 nm) of **Ir-ppy-Tz** (a), **Ir-pbt-Tz** (b), **Ir-dfppy-Tz** (c) in methanol solution (10 μM) under different oxygen levels, and (d) the emission intensity ratio of the complexes under argon to that under air.

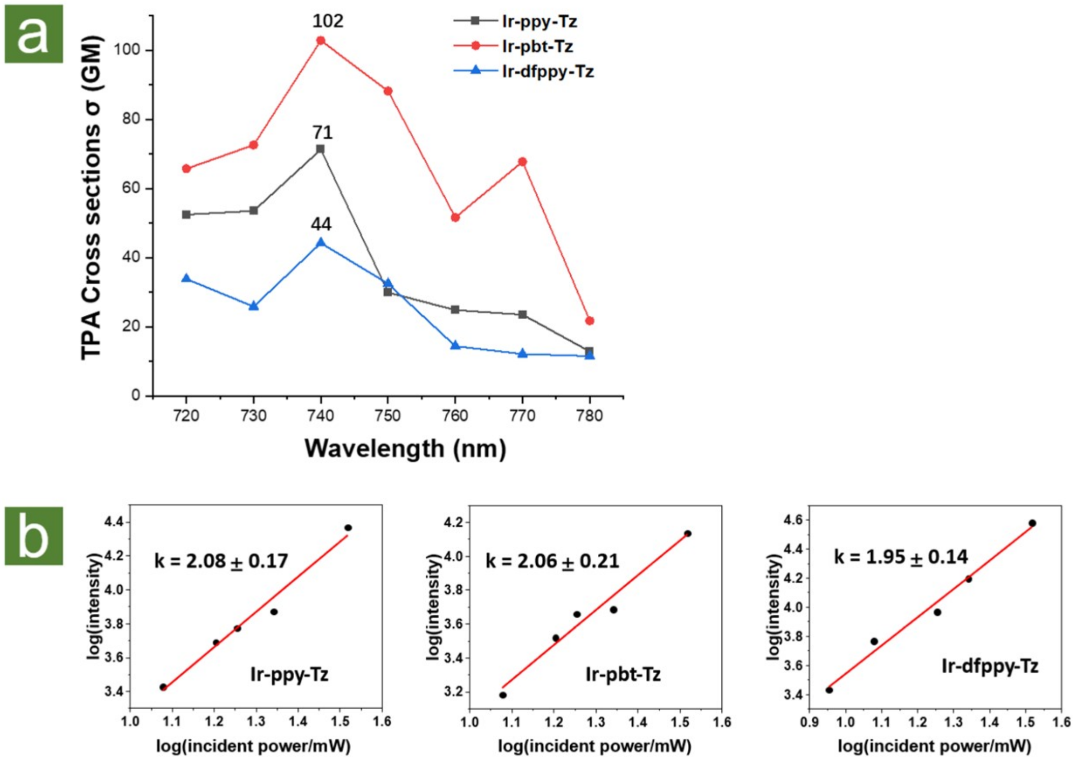

Fig. S3 (a) Two-photon absorption cross-sections of **Ir-ppy-Tz**, **Ir-pbt-Tz**, and **Ir-dfppy-Tz**, respectively, at 720 ~ 780 nm. (b) Validation of two-photon excitation by linear fitting of the logarithmic plots of the incident femtosecond laser power *versus* luminescence intensity of the compounds at 740 nm.

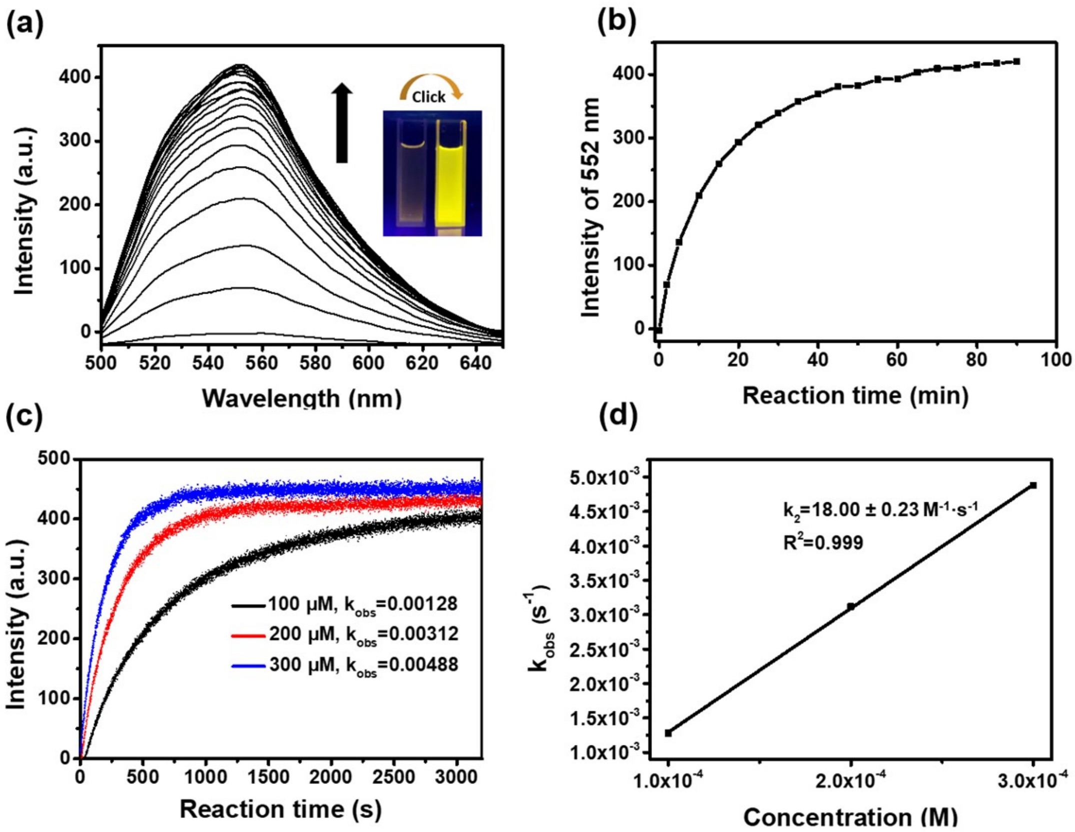

Fig. S4 The bioorthogonal reaction of **Ir-pbt-Tz** (10 μM) and BCN (100-300 μM) in methanol/water (1:1, v/v) at 298 K.

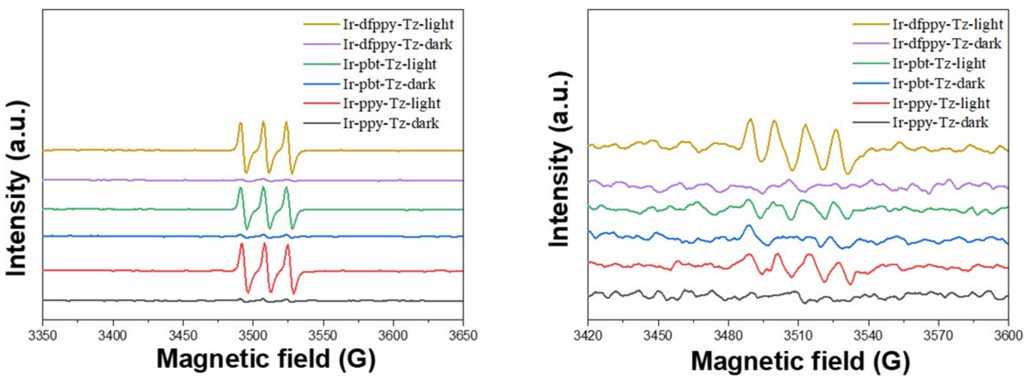

Fig. S5 ESR spectra of $^1O_2$ trapped by TEMP (left) / $O_2^{\bullet-}$ trapped by DMPO (right) in the Ir(III) complex solution with or without light input.

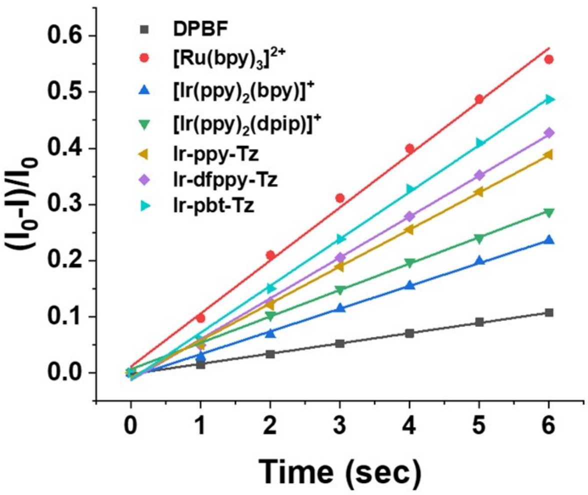

Fig. S6 Plots of the cumulative decrease in optical density of DPBF (60 μM) at 411 nm along irradiation time (λ_{irr}=405 nm) in the presence of the indicated complexes. $[Ru(bpy)_3]^{2+}$ as the standard.

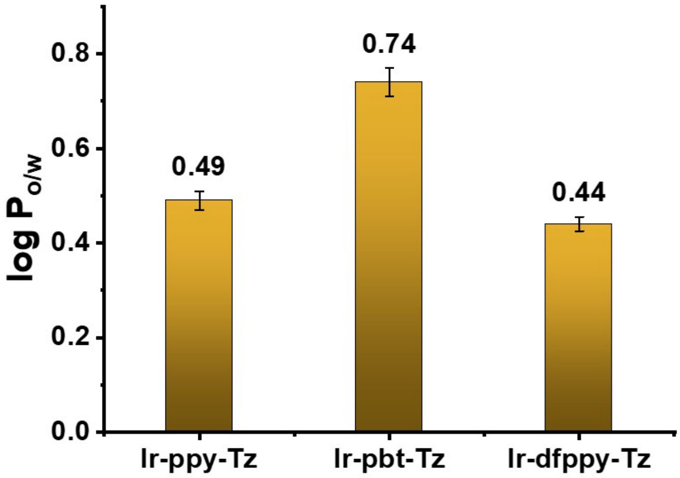

Fig. S7 Partition coefficient (log $P_{o/w}$) of the indicated complexes. All the experiments were performed as duplicates of triplicates (n = 3 independent experiments). The error bars represent the standard deviation (SD).

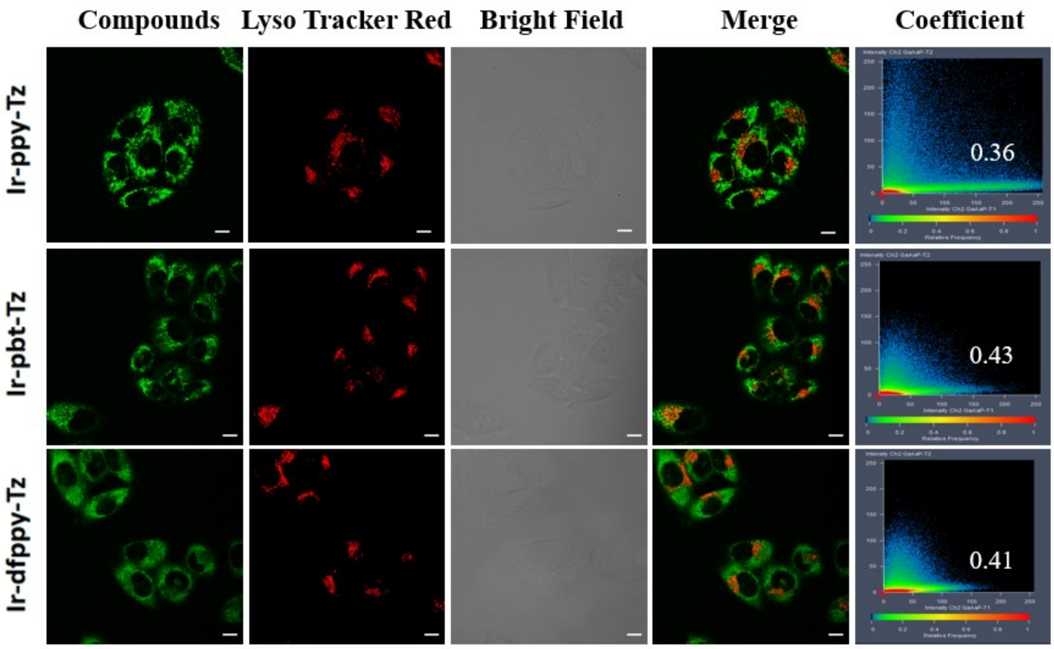

Fig. S8 CLSM imaging of A549 cells incubated with 1 μM Ir(III) complexes for 4 h at 37 °C (**Ir-ppy-Tz**: λ_{ex} = 405 nm, λ_{em} = 580 - 610 nm; **Ir-pbt-Tz**: λ_{ex} = 405 nm, λ_{em} =540 - 570 nm; **Ir-dfppy-Tz**: λ_{ex} = 405 nm, λ_{em} = 510 - 540 nm), followed by 100 nM of LysoTraker Deep Red (λ_{ex} = 633 nm, λ_{em} = 650 - 690 nm). Scale bar: 10 μm.

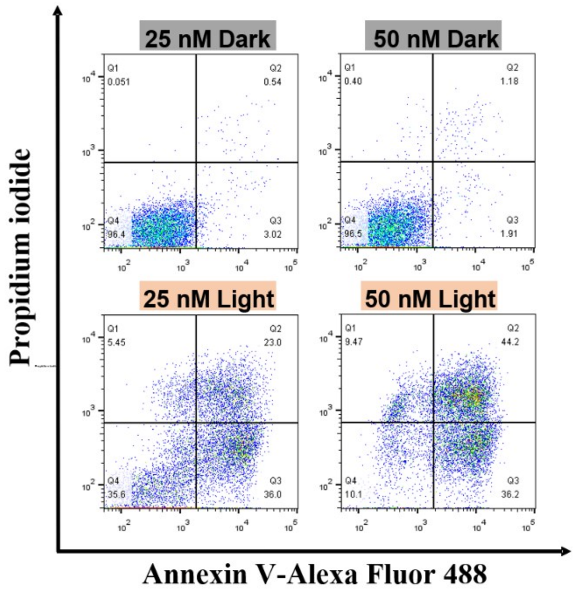

Fig. S9 Ir-pbt-Tz (50 nM, 4 h, 37 °C) concentration-dependent flow cytometry analysis of cells upon irradiation (405 nm, 20 mW·cm^{-2}, 300 s). Cells were stained by Annexin V-FITC (λ_{ex} = 488 nm) and PI (λ_{ex} = 543 nm).

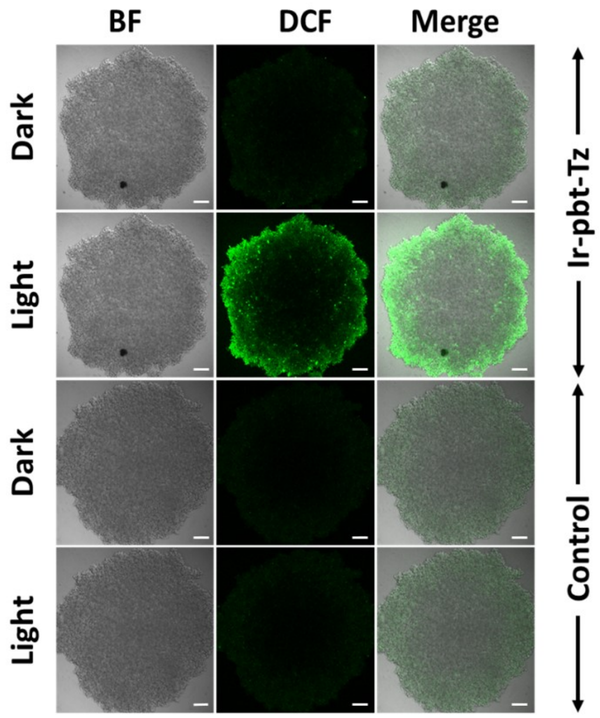

Fig. S10 CLSM imaging of ROS generation in MCTS incubated with the 1 μM DCFH-DA after pre-incubation with **Ir-pbt-Tz** (50 nM, 4 h, 37 °C) after two-photon PDT. DCFH-DA: λex = 488 nm, λem = 510 - 540 nm. Scale bar: 100 μm.

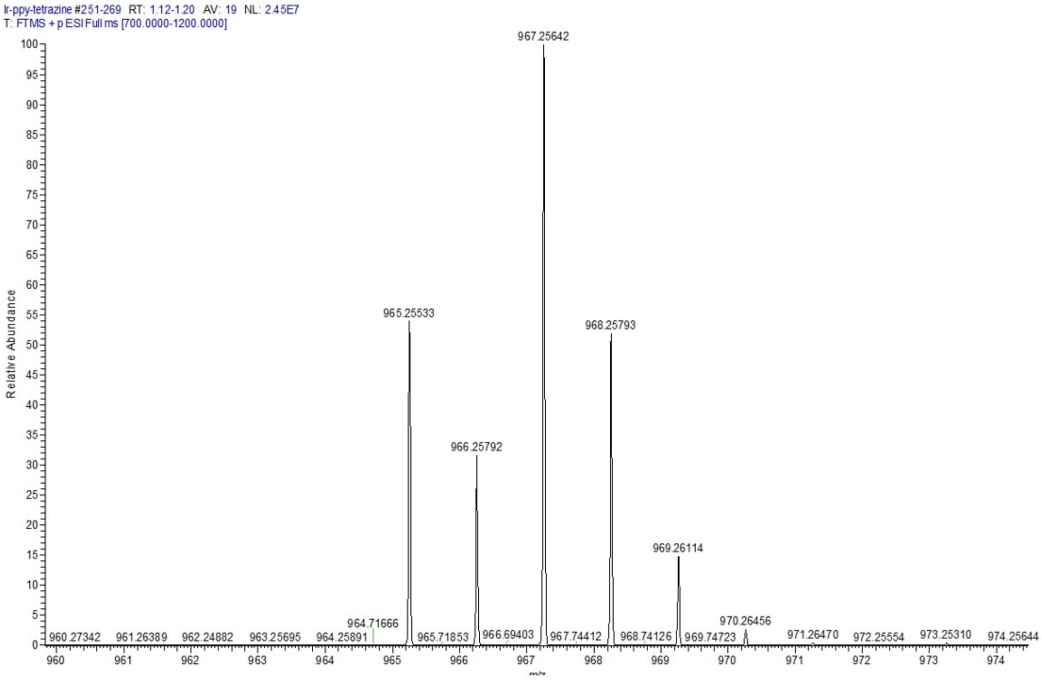

Fig. S11 HR-ESI-MS spectrum of **Ir-ppy-Tz**.

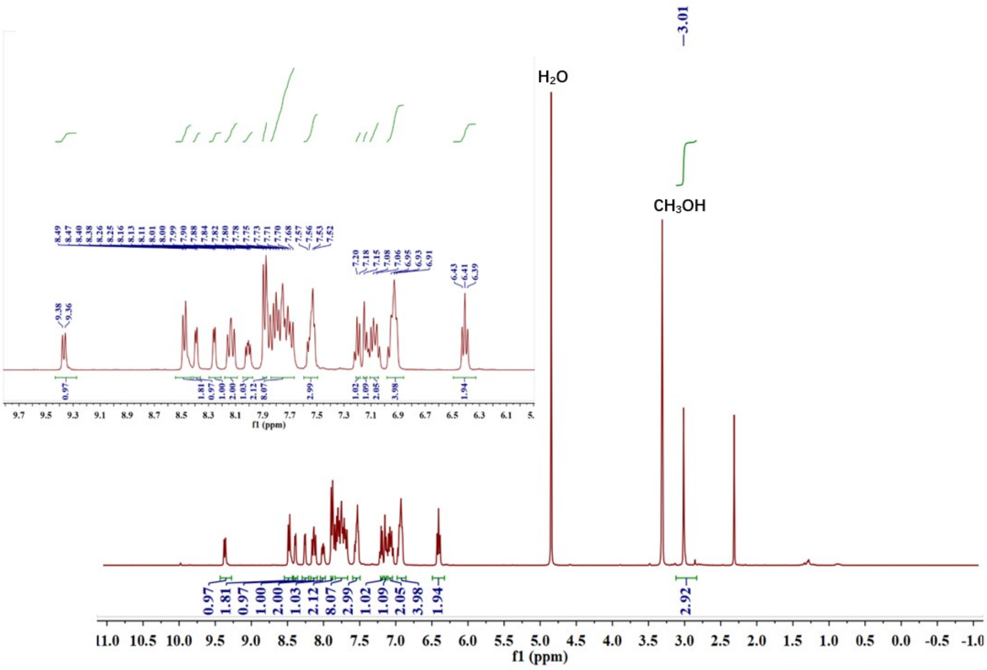

Fig. S12 ^{1}H NMR spectrum of **Ir-ppy-Tz**.

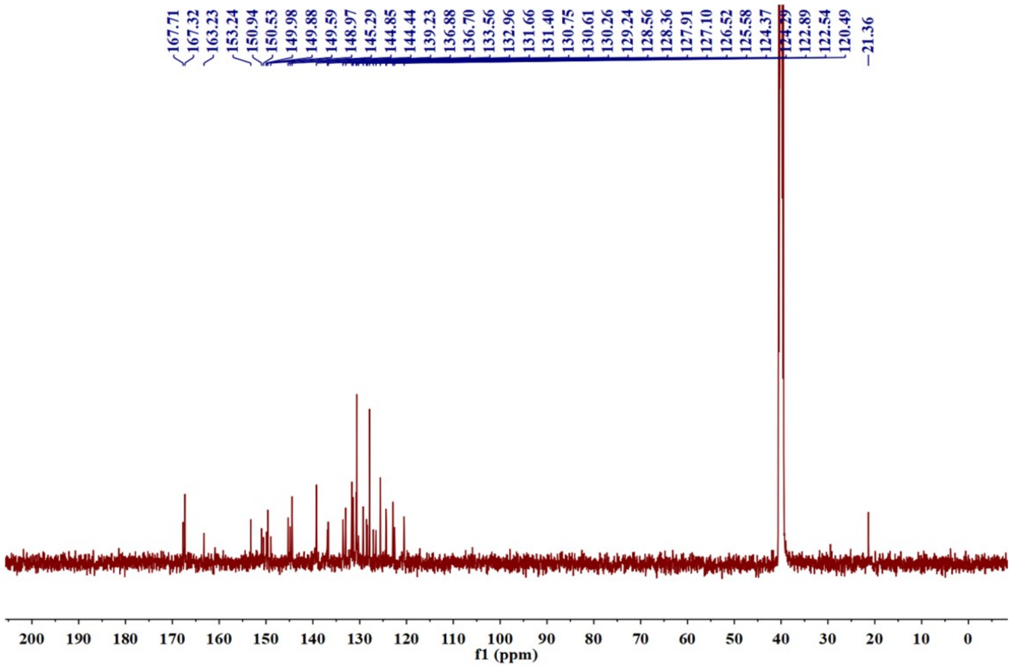

Fig. S13 ^{13}C NMR spectrum of **Ir-ppy-Tz**.

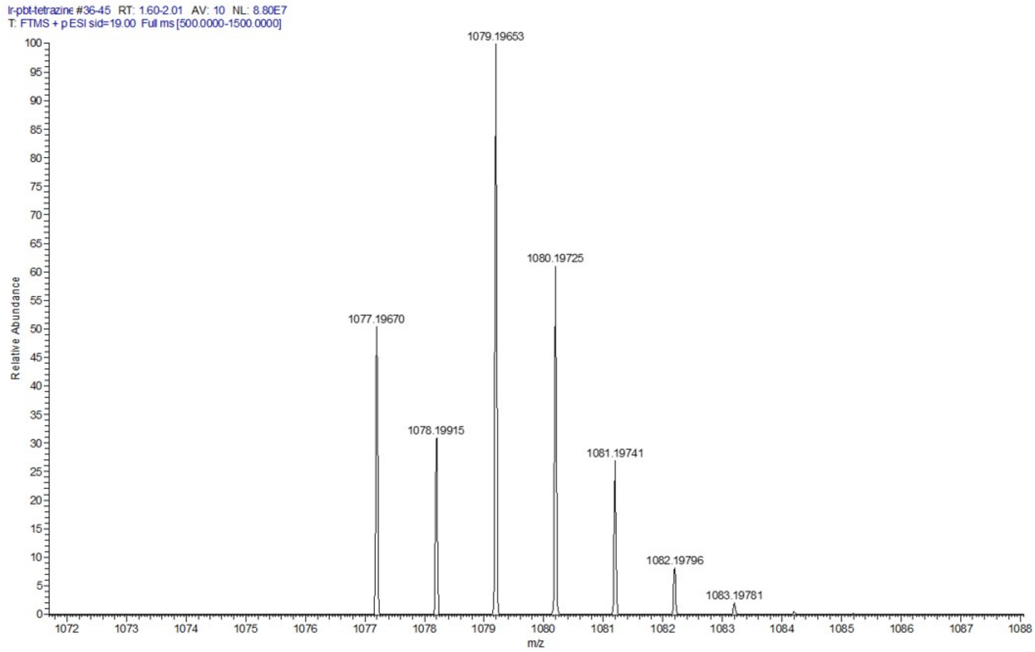

Fig. S14 HR-ESI-MS spectrum of **Ir-pbt-Tz**.

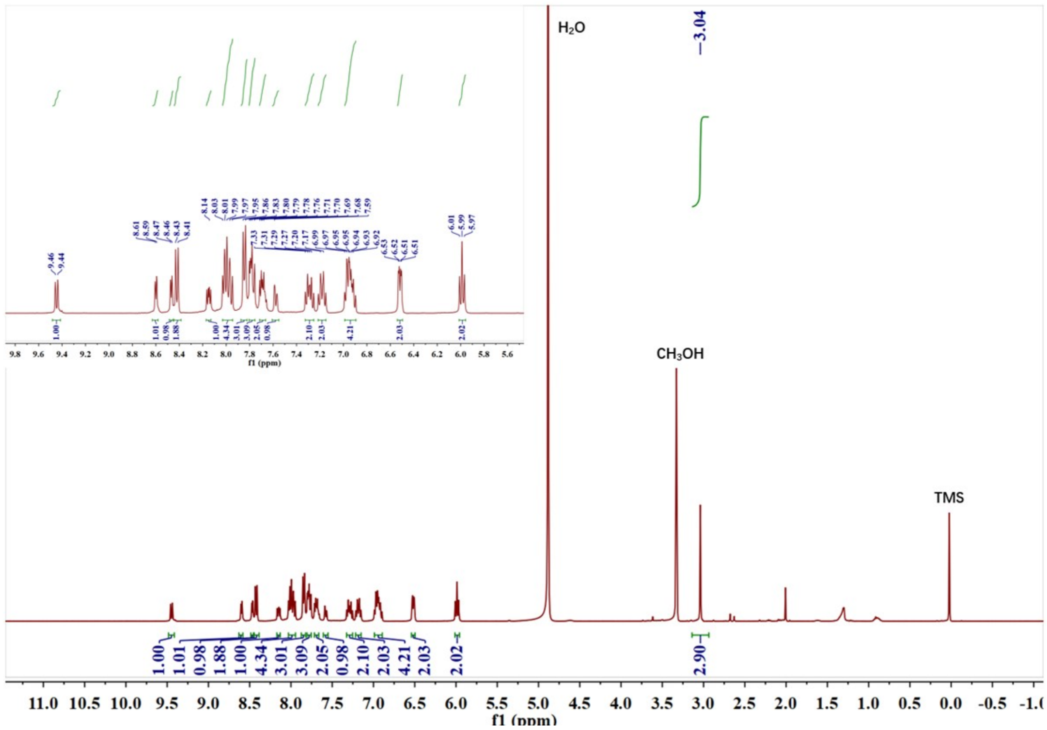

Fig. S15 ^{1}H NMR spectrum of **Ir-pbt-Tz**.

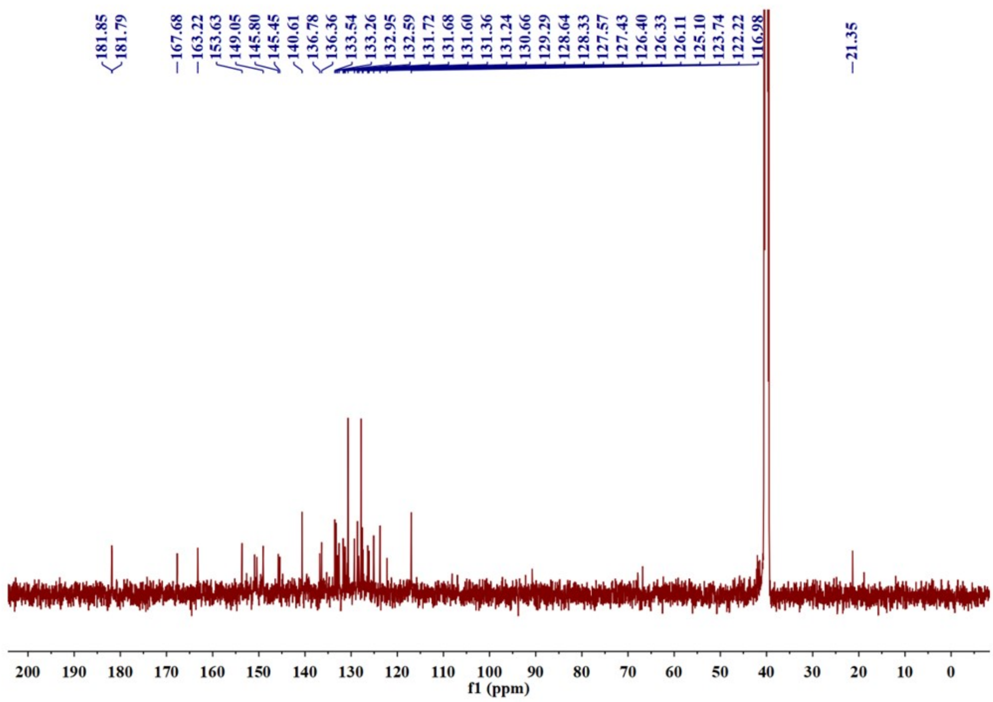

Fig. S16 ^{13}C NMR spectrum of **Ir-pbt-Tz**.

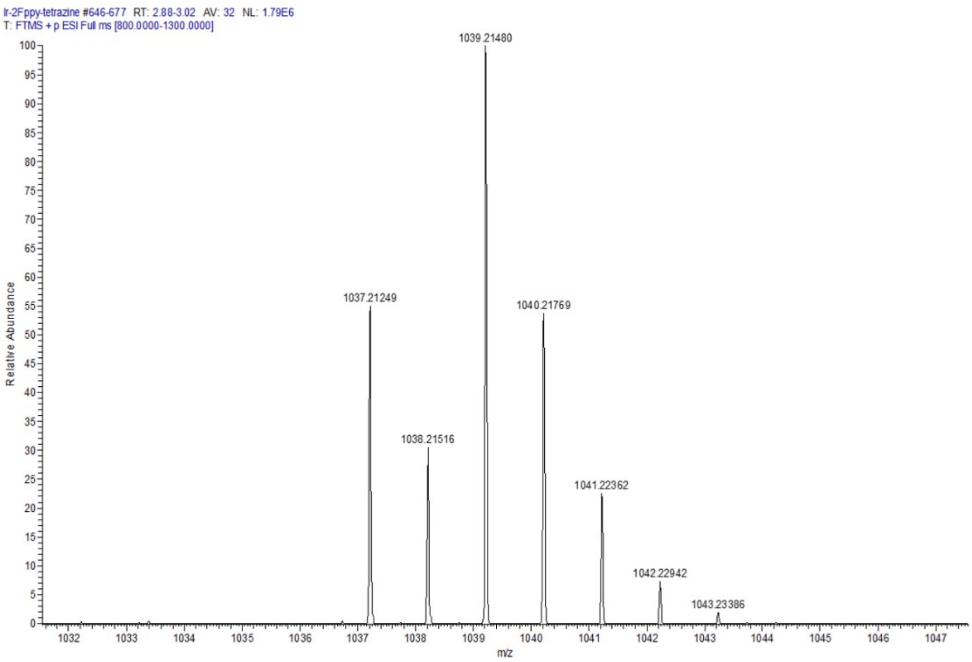

Fig. S17 HR-ESI-MS spectrum of **Ir-dfppy-Tz**.

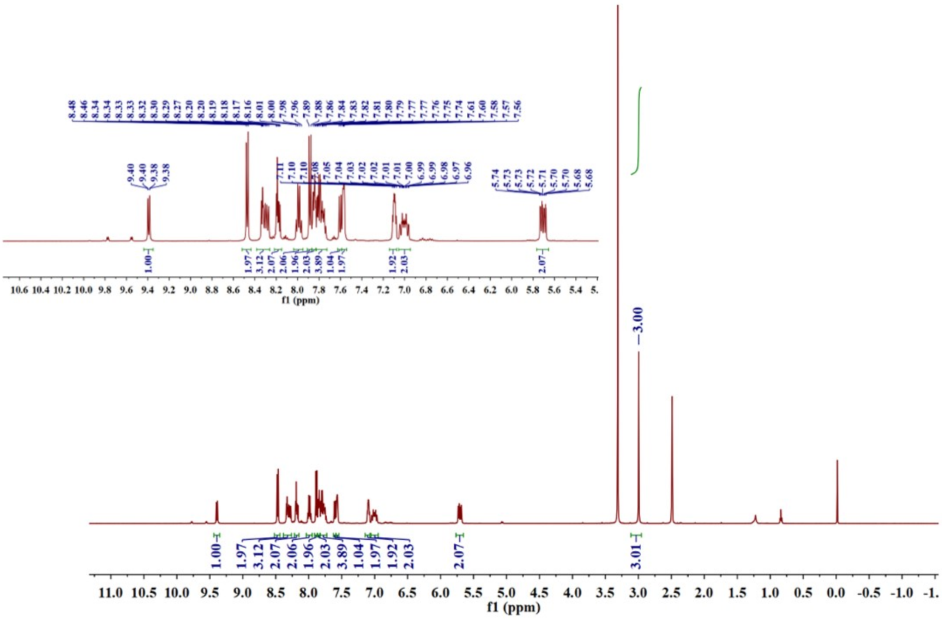

Fig. S18 ^{1}H NMR spectrum of **Ir-dfppy-Tz**.

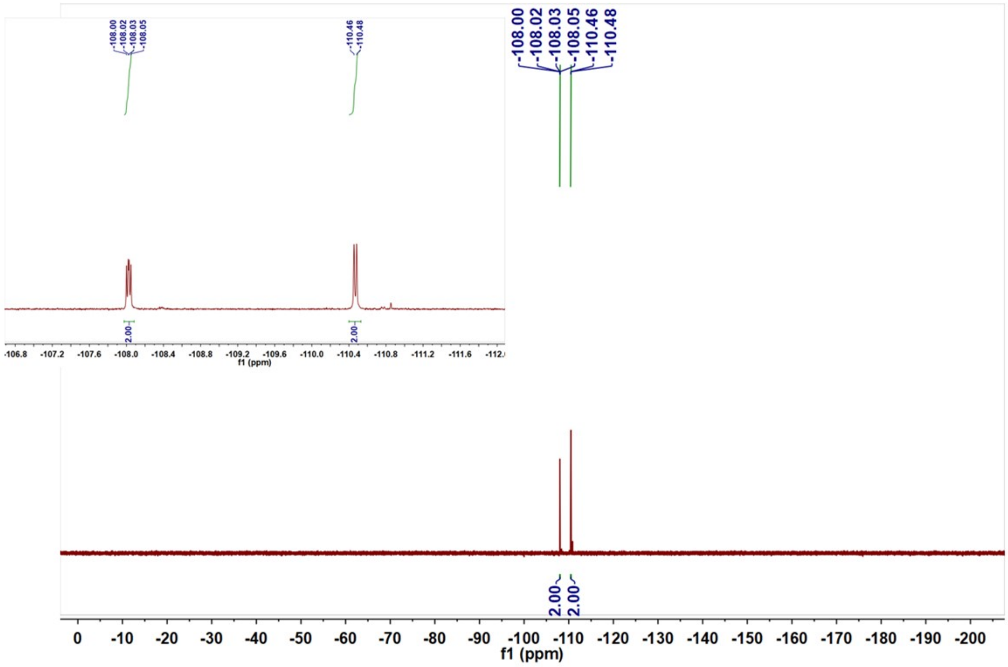

Fig. S19 ^{19}F NMR spectrum of **Ir-dfppy-Tz**.

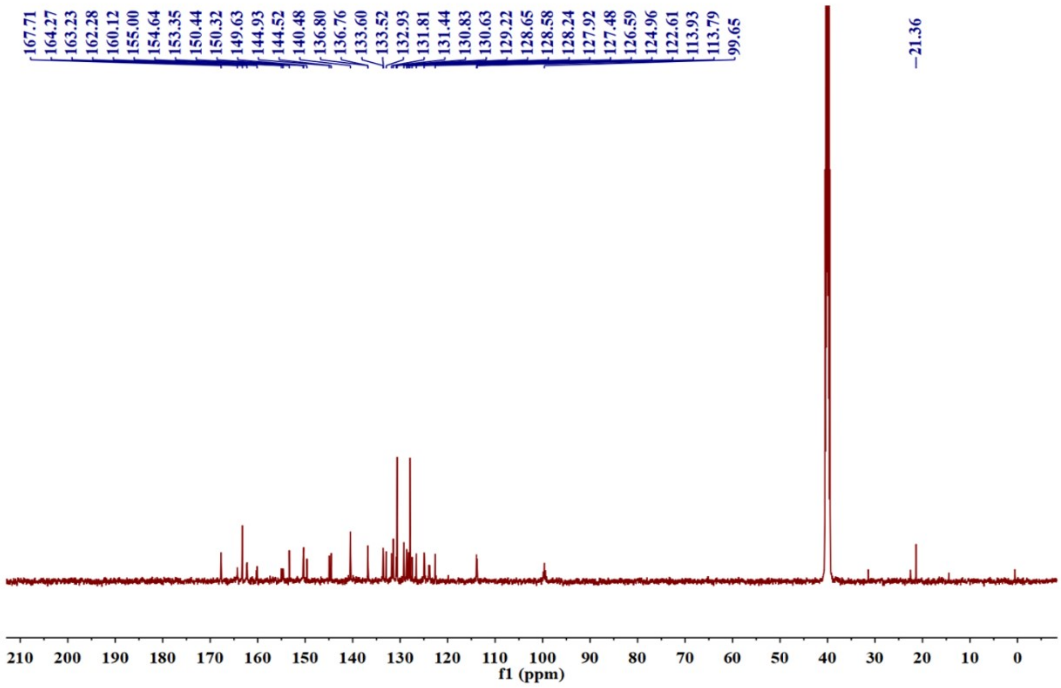

Fig. S20 ^{13}C NMR spectrum of **Ir-dfppy-Tz**.

Table S1 photophysical properties of designed compounds

Compd	λ_{abs}/nm (ε, $\times 10^3$ $M^{-1}\cdot cm^{-1}$)	$\lambda_{em/nm}$	Φ_u(air/Ar)	τ/ns
Ir-ppy-Tz	257 (54), 286 (48.9), 380 (9.9)	600	0.0101/0.0273	613
Ir-pbt-Tz	258 (60.7), 290 (72), 401 (14)	559	0.0421/0.1684	475
Ir-dfppy-Tz	256 (76.7), 290 (71.8), 379 (10.2)	527	0.0519/0.2751	577

Table S2 single oxygen quantumn yileds of complexes.

Compd	**$Ru(bpy)_3^{2+}$**	**$[Ir(ppy)_2(bpy)]^+$**	**$[Ir(ppy)_2(dpip)]^+$**
Φ_Δ	0.81	0.35	0.40
Compd	**Ir-ppy-Tz**	**Ir-pbt-Tz**	**Ir-dfppy-Tz**
Φ_Δ	0.56	0.72	0.62